

FocusGraph: Graph-Structured Frame Selection for Embodied Long Video Question Answering

Tatiana Zemskova^{1,2}, Solomon Andryushenko³, Ilya Obruchov⁴, Viktoriia Khoruzhaia², Ekaterina Eroshenko², Ekaterina Derevyanka⁴, and Dmitry Yudin^{1,2}

¹ AXXX

² MIRAI

³ Yandex

⁴ FusionBrain Lab

Abstract. The ability to understand long videos is vital for embodied intelligent agents, because their effectiveness depends on how well they can accumulate, organize, and leverage long-horizon perceptual memories. Recently, multimodal LLMs have been gaining popularity for solving the long video understanding task due to their general ability to understand natural language and to leverage world knowledge. However, as the number of frames provided to an MLLM increases, the quality of its responses tends to degrade, and inference time grows. Therefore, when using MLLMs for long video understanding, a crucial step is selecting key frames from the video to answer user queries.

In this work, we develop FocusGraph, a framework for keyframe selection for question answering over long egocentric videos. It leverages a lightweight trainable Scene-Caption LLM Selector that selects query-relevant clips based on their graph-based captions, and a training-free method for selecting keyframes from these clips. Unlike existing methods, the proposed Scene-Caption LLM Selector does not rely on the original sequence of low-resolution frames; instead, it operates on a compact textual representation of the scene. We then design a training-free Patchwise Sparse-Flow Retention (PSFR) method to select keyframes from the resulting sequence of clips, which are fed into an MLLM to produce the final answer. Together, these components enable FocusGraph to achieve state-of-the-art results on challenging egocentric long-video question answering benchmarks, including FindingDory and HourVideo, while significantly reducing inference time relative to baseline approaches.

1 Introduction

Understanding long videos is a fundamental task for embodied intelligent agents operating in real-world environments [1, 25]. Such agents must continuously perceive their surroundings, interact with objects, and reason over extended temporal horizons [5, 8]. Their performance therefore critically depends on the ability to accumulate, organize, and leverage long-term perceptual memories [16, 46]. This

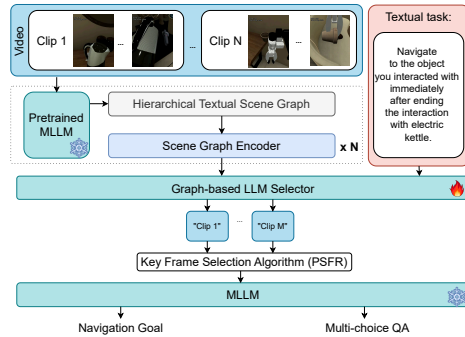


Fig. 1: We propose FocusGraph, a modular method that addresses navigation and question-answering tasks on long videos using hierarchical textual scene graphs and a training-free fast key frame selection method called PSFR.

challenge has recently gained increasing attention in long-video question answering (LVQA), where an agent answers natural language queries over potentially hours-long video streams [4, 41, 48].

Embodied videos, typically captured from an egocentric or agent-centric perspective, present unique challenges compared to conventional internet videos [6, 10]. They exhibit frequent camera motion, occlusions, viewpoint changes, and visually repetitive content [10], while the information required to answer a question may be sparsely distributed across the entire video [44]. For example, to solve the task «Navigate to the receptacle that you placed an object on right before you started interacting with the can» [44], the agent must answer the question: «What is the receptacle that you placed an object on right before you started interacting with the can?». To answer this question, the agent must be able to recognize actions, identify objects by their semantic category, and perform temporal reasoning. Beyond the challenges inherent to question answering in embodied videos, such videos also provide additional information: during recording, the camera moves through a continuous 3D space. This makes it possible to exploit the spatio-temporal coherence of observations, reconstruct the agent’s trajectory, and establish stable spatial relationships between objects and scenes over time. As a result, LVQA for embodied videos represents a particularly promising research direction that calls for the development of specialized methods.

Recent progress in multimodal large language models (MLLMs) has shown promising results for video understanding tasks, leveraging powerful natural language reasoning capabilities and world knowledge [2, 39, 51]. However, directly applying MLLMs to long videos introduces significant challenges, including sharply increased inference cost [37] and degraded answer quality as number of input frames grows for open-source models [40, 44]. These limitations arise from constrained context capacity and attention «dilution» effect, making naive scaling to long videos impractical.

Existing approaches address this problem mainly in two ways: either by compressing the visual representation of individual frames to reduce the number of tokens [13, 21, 22, 32, 52], or by selecting a subset of query-relevant frames [19, 20, 34, 35, 49, 53]. However, visual feature compression inevitably leads to information loss, while frame selection requires a well-designed retrieval strategy, particularly in scenarios where answering a question depends on the full long-term context of the video. As a result, two-stage methods appear especially promising: in the first stage, a coarse frame selection is performed using an MLLM operating on a compressed scene representation, followed by a more detailed analysis of the selected segments in the second stage. Nevertheless, existing two-stage approaches [38, 43, 47] treat video as a sequence of images constraining the maximum number of frames and events that an MLLM can process as input, while additionally reducing computational efficiency and overall inference speed.

In this work, we address these challenges by introducing an efficient, query-aware framework for long-video question answering in embodied settings. Motivated by the strong redundancy in long embodied videos and the localization of relevant information to a few semantically meaningful moments, we decouple long-video understanding into two complementary stages: (1) lightweight, query-relevant clip selection trainable model, and (2) training-free identification of key frames in the selected clips.

Unlike prior frame selection approaches, our frame selector operates on a compact scene caption representation rather than raw low-resolution frame sequences. This representation encodes objects, interactions, and their temporal relationships, enabling efficient long-horizon reasoning with reduced computational cost. The selected clips are converted into a sequence of frames, some of which contain redundant information. To extract key frames from these clips, we introduce a fast, training-free algorithm for key frame selection based on tracking changes in the image sequence. By combining graph-based temporal abstraction with query-conditioned selection and optical flow for key frame extraction, our method achieves both accuracy and efficiency.

We evaluate the proposed approach on challenging egocentric LVQA benchmarks, including FindingDory and HourVideo, where questions require long-horizon reasoning and precise temporal grounding. Our method achieves state-of-the-art performance on these benchmarks while substantially reducing inference time compared dense frame processing baselines.

In summary, our contributions are the following:

- We propose FocusGraph, a novel framework for embodied videos that combines query-conditioned clip selection with training-free key frames identification based on Patchwise Sparse-Flow Retention algorithm (PSFR).
- We introduce a hierarchical textual graph-based scene representation for efficient long-horizon reasoning, enabling lightweight and scalable frame selection independent of raw frame sequences.
- We demonstrate state-of-the-art performance and improved inference efficiency on challenging egocentric long-video question answering benchmarks.

Our results highlight the importance of selective temporal abstraction and structured representations for effective long-video question answering in embodied environments.

2 Related works

MLLMs for Long Video Understanding. Long-form video understanding has emerged as a central challenge in multimodal reasoning, as increasing video length leads to higher inference costs and degraded performance in visual language models due to limited context capacity and difficulty modeling long-range dependencies. To mitigate these issues, prior work has explored strategies for representing long videos while preserving salient information, which broadly fall into frame sequence compression, scene representation augmentation, and key frame selection. Compression-based methods reduce input length or dimensionality through techniques such as fusing frames into panel-like grids [18], merging or pruning visual tokens based on multimodal importance [54], or leveraging codec-aware signals to construct compact semantic representations [14], though these approaches often discard fine-grained visual details critical for reasoning. Scene augmentation methods introduce additional temporal or semantic cues, such as detailed scene annotations in RoboAnnotatorX [17] or explicit time markers in DATE [49], improving temporal localization at the cost of either information loss from textual replacement or sustained computational burden when full visual content is retained. In contrast, our approach unifies scene representation augmentation and key frame selection in a two-stage, question-aware framework that jointly leverages intrinsic video structure and query semantics to efficiently retain the most relevant visual information.

LLM-free keyframe selection. Recent work improves long-video understanding without finetuning by inserting a lightweight selection stage before a frozen Video-LLM. Methods split into query-conditioned and query-agnostic selection. Query-conditioned approaches optimize relevance for video QA but require the query in advance: AKS [35] adaptively splits timelines using cheap VLM scoring, while Q-Frame [53] samples query-aware frames across multiple temporal resolutions under a token budget. Query-agnostic methods are reusable across queries and suitable for streaming or multi-turn settings, typically optimizing general criteria such as diversity, motion, or information content. Examples include semantic and motion-aware frame selection with auxiliary cues (See&Trek [19], StimuVAR [12]), redundancy reduction via embedding-space volume maximization (MaxInfo [20]), memory-aware importance estimation for streaming (StreamMem [45]), and efficient two-stage relevance estimation exploiting temporal redundancy (FOCUS [55]), though the latter is limited by reliance on semantic similarity rather than higher-level reasoning. However, the training-free approaches estimate relevance primarily from low-level or semantic similarity signals and therefore remain limited in tasks requiring compositional or higher-level reasoning. In contrast, we integrate a training-free keyframe selection stage after the reasoning step over a compressed video representation. This

allows us to employ a fast algorithm that relies solely on lightweight visual image features, is inexpensive to compute, and is well suited to embodied settings.

LLM-based keyframe selection. Recent research on retrieval-augmented generation (RAG) for embodied and video understanding can be broadly divided into training-free and training-based approaches. Training-free methods, such as Embodied-RAG [42], AKeyS [7] and ReMEmbR [1], rely on non-parametric or explicitly constructed spatio-temporal memories, offering strong flexibility and ease of adaptation without additional optimization. Logic-in-Frames [11] introduces dynamic keyframe search with visual semantic-logical verification with graph-based representation of a question. However, these approaches often struggle with queries that require reasoning over the entire video context. For example, to answer questions like *"What is the object that you manipulated the second time?"* such approaches may resort to agentic or iterative retrieval strategies, significantly increasing inference cost [1]. In contrast, training-based approaches learn task-specific retrieval or temporal grounding strategies, enabling more efficient inference. Representative examples include generative frame sampling [47], reinforcement-learning-based temporal grounding [43], instructed temporal grounding in multimodal settings [38]. These methods explicitly model temporal dependencies and reasoning signals, allowing them to better capture long-range video semantics while maintaining computational efficiency. Motivated by this trade-off, we adopt a training-based RAG perspective and propose a graph-based representation of the video to improve the speed efficiency of our LLM-based keyframe selection pipeline. However, unlike existing methods that operate on sequences of low-resolution images, our approach works with a compressed scene representation in the form of graph sequences.

Scene graphs for Video Question Answering. Recent works in video question answering focuses on augmenting scene representations with additional modalities, most commonly text. The textual scene representation is often structured as a graph, which has been shown to enhance compositional reasoning and improve question-answering performance. Recent methods leverage spatio-temporal or action-centric scene graphs to capture object interactions and temporal dynamics in videos, enabling more structured reasoning over long horizons, as demonstrated in the work of Mao et al. [27], STEP [29], HyperGLM [28], and action scene graph-based approaches [30]. Scene graph representations have also been used to accelerate long-video understanding via compressed or graph-enabled chain-of-thought reasoning [23], as well as to support zero-shot video QA through temporally structured triplets [56]. However, the quality of the answers remains highly dependent on the accuracy and stability of the predicted scene graphs. Most existing approaches rely on per-frame or densely sampled scene graph prediction, which can lead to unstable graph sequences in settings with moving robotic cameras and excessive graph lengths for long videos, as further highlighted by methods that encode long sequences of textual scene graphs [24]. To address these limitations, we propose generating scene graphs at the clip level, which yields more stable representations and improves both the quality and efficiency of video description generation.

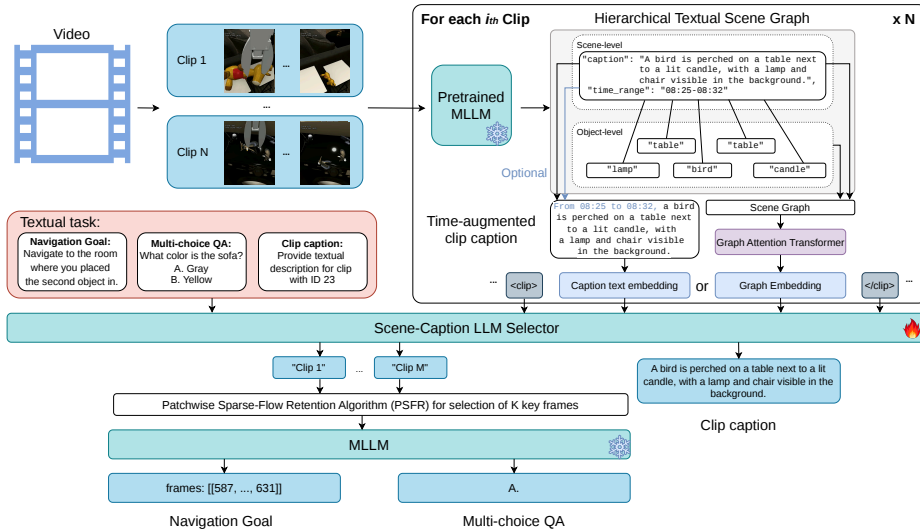


Fig. 2: FocusGraph overview. FocusGraph takes egocentric video as input and splits it into clips with a fixed number of frames. Then, for each clip, a pretrained MLLM constructs an object-centric representation of the scene in the form of a hierarchical textual scene graph, containing a list of objects and a scene description. We also store the time range of the original video from which a clip is extracted. Next, a time-augmented clip caption is generated from each graph-based clip description, which is then projected into the Scene-Caption LLM Selector. The Scene-Caption LLM Selector selects the clips that contain the answer to the question. From the selected clips, K key frames are chosen using the proposed training-free PSFR algorithm. The K key frames are then fed into an MLLM, which uses them to solve various tasks, such as navigation goal selection (FindingDory) or multi-choice question answering (HourVideo).

3 Method

Overview. When developing the method, our goal is to create an approach that can quickly extract from a video the information relevant for answering a question, while being able to handle different types of questions and take into account the full context of the agent’s observation history.

Overview of the proposed FocusGraph framework is presented on Fig. 2. FocusGraph takes an egocentric video as input and decomposes it into a sequence of clips, each containing a fixed number of frames. For each clip, a pretrained multimodal large language model (MLLM) constructs an object-centric representation of the scene in the form of a textual graph, which includes a list of detected objects along with a high-level scene description. The temporal range of the original video corresponding to each clip is also recorded. We detail this process in Sec. 3.1. The resulting sequence of graph-based clip descriptions is then transformed into time-augmented clip captions and passed to the Scene-Caption LLM Selector, whose role is to identify the subset of clips that are most

relevant for answering a given query. This selection step enables efficient reasoning over long egocentric videos by filtering out irrelevant content (details are provided in Sec. 3.1). From the selected clips, we further extract K key frames using the proposed training-free PSFR algorithm detailed in Sec. 3.4. These key frames serve as a compact yet informative visual summary of the relevant video segments. Finally, the selected key frames are fed into an MLLM, which performs downstream tasks such as navigation goal selection in FindingDory or multi-choice question answering in HourVideo.

We train the Scene-Caption LLM selector using supervised fine-tuning on the GenS-Video-150K dataset, which contains annotations of frames relevant to answering the question. During training, the Scene-Caption LLM selector learns both to predict a list of the most relevant clips for answering the question and to decode a clip description from its compressed representation, enabling it to learn more stable projections of textual embeddings. Details of the training process are provided in Sec. 3.3. To optimize the PSFR hyperparameters, we use program evolution of the keyframe selector function, leveraging ground-truth frame annotations from the GenS-Video-150K and FindingDory datasets (see Sec. 3.5).

3.1 Clip-level Scene Graph Construction.

To ensure that our method generalizes to diverse egocentric videos, we employ an MLLM to construct a scene graph representation. Egocentric videos captured by a moving camera often contain viewpoints in which objects are partially occluded or poorly distinguishable. To mitigate this issue, we aggregate information across multiple consecutive frames and build a unified graph representation for a short temporal segment.

Formally, let the input video be denoted as $V = \{f_t\}_{t=1}^T$, where f_t is the video frame at time index t , and T is the total number of frames. We partition V into N non-overlapping clips $\mathcal{C} = \{C_i\}_{i=1}^N$, where each clip $C_i = \{f_{(i-1) \cdot n+1}, \dots, f_{i \cdot n}\}$ contains a fixed number of frames n_{frames} .

Each clip C_i is provided as input to the multimodal model Qwen2.5-VL-7B-Instruct [36]. The model produces a textual representation: $\mathcal{T}_i = (\mathcal{O}_i, d_i)$, where \mathcal{O}_i is the set of objects and subjects (e.g., robots or people), and d_i is a natural-language sentence describing the overall scene and ongoing actions within the clip as well as spatial relations between objects. This textual output constitutes a clip-level scene graph.

If the dataset includes absolute recording timestamps, we associate each scene description d_i of i th clip with a temporal interval $\tau_i = [t_i^{\text{start}}, t_i^{\text{end}}]$, where t_i^{start} and t_i^{end} denote the start and end times of the clip, respectively.

An example of an extracted clip-level graph is shown in Fig. 2. The system prompt used for clip graph extraction is provided in the Appendix.

3.2 Scene-Caption LLM Selector.

To provide the sequence of clip-level scene captions as input to a Large Language Model (LLM), we convert them into a sequence of continuous embeddings aligned with the LLM embedding space. The tokenization procedure is designed to be both compact and information-preserving.

Initial text embeddings. For each clip C_i , we embed textual representations \mathcal{T}_i using ModernBERT-large. Let $\phi(\cdot) : \text{text} \rightarrow \mathbb{R}^{D_{\text{in}}}$ denote this embedding function. If the dataset provides annotated time ranges, we first augment the caption with the corresponding temporal interval (i.e., we append the time range to the caption text), and then extract the textual embedding of this time-augmented caption. Formally, for a clip C_i , we obtain a clip-level caption embedding $\mathbf{c}_i = \phi(\tilde{d}_i) \in \mathbb{R}^{D_{\text{in}}}$, where \tilde{d}_i denotes the original caption d_i augmented with its associated time range when such annotation is available (otherwise, $\tilde{d}_i = d_i$).

Projection to LLM embedding space. Since the LLM operates in a different embedding space of dimension D_{LLM} , we align caption embeddings using lightweight adapter networks. The caption embedding is defined as $\mathbf{z}_i^{\text{cap}} = f_{\text{cap}}(\mathbf{c}_i) \in \mathbb{R}^{D_{\text{LLM}}}$.

Video token sequence construction. Let $\mathbf{E}_i^{\text{text}} \in \mathbb{R}^{L_i \times D_{\text{LLM}}}$ denote the standard LLM token embeddings of the textual prompt corresponding to clip C_i . The text prompt consists of the special tokens `<clip>` and `</clip>` that mark the beginning and end of the clip. The final scene embedding sequence is constructed by interleaving text tokens with graph-based tokens in temporal order:

$$\mathbf{E} = [\mathbf{E}_1^{\text{text}}, \mathbf{z}_1^{\text{cap}}, \dots, \mathbf{E}_{N-1}^{\text{text}}, \mathbf{z}_{N-1}^{\text{cap}}, \mathbf{E}_N^{\text{text}}]. \quad (1)$$

This fully vectorized sequence is directly provided to the LLM, enabling seamless integration of the compressed scene caption information into autoregressive language modeling without modifying the LLM architecture.

3.3 Training Procedure.

We train the Scene-Caption LLM Selector on the GenS-Video-150K dataset [47], which contains dense fine-grained annotations of frames relevant for answering questions. It includes videos from the YT-Temporal-1B dataset [50], which consists of YouTube videos from diverse sources. We use this dataset because it provides a large amount of data across different domains. For each question, we retain the top-8 most relevant clips to improve the model’s inference speed. We exploit this supervision to perform standard full-parameter supervised fine-tuning (SFT). Specifically, we jointly fine-tune: (i) the Large Language Model (LLM), (ii) text embedding adapters that project textual embeddings into the LLM latent space. As an auxiliary training objective, we use a clip caption reconstruction task based on its clip ID. This encourages the model to learn text embedding adapters that accurately project the semantic content of textual embeddings into the LLM latent space.

During this stage, optimization is performed using the token-level cross-entropy loss:

$$\mathcal{L}_{\text{SFT}} = - \sum_{t=1}^T \log p_{\theta}(y_t | y_{<t}, x), \quad (2)$$

where y_t denotes the ground-truth token at time step t , $y_{<t}$ represents the preceding tokens, x is the multimodal input, and θ are the model parameters.

3.4 Patchwise Sparse-Flow Retention (PSFR)

The Scene-Caption LLM selector chooses M clips that contain the answer to the question. Since compressing a video into a sequence of clip-level scene representations inevitably leads to some information loss, we feed frames from the selected clips into an MLLM to refine the answer using the full visual information. As each clip contains n_{frames} frames, we aim to select key frames that do not duplicate other frames in the sequence.

For this purpose, we propose a training-free, two-stage keyframe selector inspired by the pixel-tracking branch of FlowGEBD [9], but implemented using sparse optical flow only. During the first stage the keyframe selector detects moments of strong structural change by monitoring patchwise corner-track retention. The second stage turns these streaming statistics into a fixed-budget, diversity-aware keyframe set for VLM question answering. Full details and ablations are deferred to the appendix.

First stage. Let $\{I_t\}_{t=0}^{T-1}$ be frames after optional deterministic resizing to (W, H) . We partition each frame into a regular grid of patches $\mathcal{G} = \{g_j\}_{j=1}^{N_g}$, where N_g is the number of patches, optionally augmented with centroidal patches that straddle boundaries. At the most recent reseed time τ , we maintain a set of Shi–Tomasi corners [33] $P^{\tau} \subset \mathbb{R}^2$ and per-patch denominators $n_j^{\tau} = |\{p \in P^{\tau} : p \in g_j\}|$, $j = 1, \dots, N_g$.

Corners are seeded per patch, keeping up to m points per patch and capping the global set size by C via response-based sorting and local deduplication within radius ρ . Between I_t and I_{t+1} we track corners using pyramidal Lucas–Kanade method [26] and accept tracks T^{t+1} that are successfully and reliably tracked, $T^{t+1} = \{\hat{p}_i | i \in \mathcal{S}_{t \rightarrow t+1}\}$, where $\mathcal{S}_{t \rightarrow t+1}$ are indices of surviving tracked points.

For each patch with $n_j^{\tau} > 0$, we compute a retention ratio using the count of surviving tracked points inside the patch,

$$r_j^{t+1} = \frac{c_j^{t+1}}{n_j^{\tau}}, \quad c_j^{t+1} = |\{\hat{p} \in T^{t+1} : \hat{p} \in g_j\}|. \quad (3)$$

We then count low-retention patches and trigger a PSFR event when many patches lose their tracks,

$$L^{t+1} = |\{j : n_j^{\tau} > 0, r_j^{t+1} < \tau_r\}|, L^{t+1} \geq k_{\min} \Rightarrow I_{t+1} \text{ is a PSFR event.} \quad (4)$$

If I_{t+1} is a PSFR event, we reseed denominators by setting $\tau \leftarrow t+1$ and forming P^{t+1} from the surviving tracks T^{t+1} topped up with newly detected

corners on I_{t+1} , capped at C with deduplication radius ρ . If I_{t+1} is not an event, we still refresh P^{t+1} in the same manner but keep the denominators $\{n_j^\tau\}_{j=1}^{N_g}$ from the last reseed time.

Stage 2. We extract an ordered set of K keyframes $\mathcal{K}_{\text{final}} = \{t_1 < \dots < t_K\}$ by computing simple per-frame cues, including total corner count c_t , central-window corners z_t , edge density e_t (Canny [3]), grayscale entropy h_t , a coarse motion magnitude m_t from Lucas–Kanade tracks, and the low-retention count L_t from (4). We combine them into a normalized quality score that highlights informative content and scene changes. Candidate keyframe slots are determined using cumulative content-change and quality signals, optionally aligned to strong scene-change peaks. Frames are then selected in each slot to maximize a combined score that accounts for quality, scene relevance, and diversity, with non-maximum suppression to avoid redundancy. The exact form of the keyframe selection function is determined during program evolution based on computed scores (see Sec. 3.5). We provide the detailed description of the keyframe selection function in the Appendix.

3.5 Program-evolution setup for keyframe selector search

We develop and stress-test keyframe selection strategies using an automated program-evolution loop based on OpenEvolve [31]. The goal is to optimize the mapping from precomputed per-frame signals to a discrete set of keyframe indices under a hard runtime budget.

For each video we precompute lightweight per-frame signals once and cache them. For frame t we store a feature vector $\mathbf{s}_t \in \mathbb{R}^5$ and an HSV histogram descriptor $\mathbf{h}_t \in \mathbb{R}^{432}$. The score vector concatenates robustly normalized cues derived from sparse tracking and low-level appearance, $\mathbf{s}_t = [\tilde{c}_t, \tilde{z}_t, \tilde{e}_t, \tilde{H}_t, \tilde{L}_t]$, where \tilde{c}_t is the normalized number of tracked corners, \tilde{z}_t is the normalized number of corners in a central window, \tilde{e}_t is the normalized Canny edge density [3], \tilde{H}_t is the normalized grayscale entropy, and \tilde{L}_t is the normalized count of low-retention patches from PSFR. Histograms are L2-normalized so that cosine similarity is well-defined.

For an instance q we denote the stacked arrays as $S_q \in \mathbb{R}^{T_q \times 5}$ and $H_q \in \mathbb{R}^{T_q \times 432}$. We also store the candidate index set A_q produced by the Scene-Caption LLM Selector.

Each candidate program implements a single function $\text{select}(S_q, H_q, A_q, K) \rightarrow S_q^*$, where S_q^* is a list of 0-based indices. The selector must satisfy $S_q^* \subseteq A_q$ and $|S_q^*| \leq K$. We enforce a strict CPU-only execution budget of 15 seconds per instance and set $K = 16$.

We evaluate candidates against the FindingDory frame annotations using the inclusion oracle metric defined in Equation (5). We remove instances with missing supervision. We also guard against invalid outputs by returning zero score if the selector fails, returns indices outside A_q , or violates the budget constraints.

The inclusion scores measures whether the selector retrieves at least one piece of evidence for each valid ground-truth set,

$$\text{Incl}(q) = \min_{m \in \{1, \dots, M_q\}} \mathbb{I}[|S_q \cap G_{q,m}| > 0]. \quad (5)$$

To discourage selectors that run near the time limit, we combine inclusion with a smooth time penalty. For instance q with runtime t_q and budget cap T_{\max} we use

$$\phi(t_q) = \exp\left(\log(\alpha) \cdot \text{clip}(t_q/T_{\max}, 0, 1)^\gamma\right), \quad (6)$$

where $\alpha \in (0, 1]$ controls the maximum penalty at the cap and γ controls curvature. In our experiments $T_{\max} = 15$ seconds, $\alpha = 0.95$, and $\gamma = 1$. The optimized objective is

$$J = \frac{1}{N} \sum_{q=1}^N \text{Incl}(q) \phi(t_q). \quad (7)$$

The initial program is a uniform sampler over the candidate set A_q . If $|A_q| \leq K$ it returns A_q . Otherwise it returns K indices at evenly spaced ranks in the sorted A_q list. This baseline matches the typical usage pattern of uniform subsampling while respecting the candidate clips.

We use a program-evolution engine that iteratively proposes new Python implementations of `select` and evaluates them with the objective in Eq. (7). The search maintains a population and an archive of top-performing programs. It uses multiple islands to promote diversity and periodically exchanges elite candidates.

This automated setup is used for rapid ablations and for discovering improved selection heuristics under a fixed interface and strict runtime constraints. It does not change the downstream QA model.

4 Experiments

Datasets. We evaluate our model on two challenging benchmarks for embodied long-video understanding: FindingDory [44] and HourVideo [4]. FindingDory consists of videos capturing the execution of mobile manipulation tasks, recorded in the Habitat simulator within HSSD scenes [15]. We report results on both the full validation split of FindingDory and a development subset derived from it. The development split contains 211 questions corresponding to episodes 2, 5, 6, and 9, and is used to enable direct comparison with prior work requiring a large amount of computational resources. This allows us to compare our non-agent-based approach FocusGraph with a diverse set of baselines, including agentic methods. HourVideo comprises long-form egocentric videos sourced from the Ego4D dataset [10]. For HourVideo, we use the standard development split, which includes 50 videos and a total of 1,182 questions.

Baselines. We compare our method against a diverse set of representative baselines covering both LLM-based and training-free approaches. GenS [47] and

Table 1: Performance comparison across frame sampling methods and LLM settings (Finding Dory).

Frame Selection Method	QA LLM	Frame number	All tasks		Single-Goal Spatial Tasks		Single-Goal Temporal Tasks		Multi-Goal Tasks	
			full val.	dev.	full val.	dev.	full val.	dev.	full val.	dev.
Uniform Sampling	Gemini-2.0-Flash	96	25.73	-	31.5	-	25.0	-	8.8	-
Uniform Sampling	GPT-4o	96	27.33	-	30.9	-	31.4	-	6.5	-
Uniform Sampling	Gemini-3-Flash	8	-	26.42	-	31.82	-	30.60	-	2.1
Uniform Sampling	GPT-5-Mini	8	-	26.82	-	28.36	-	38.99	-	2.8
Uniform Sampling	Qwen-2.5-VL-7B	8	12.6	18.4	16.4	22.6	11.8	19.4	2.0	3.2
MaxInfo	Qwen-2.5-VL-7B	16	13.7	17.2	17.5	19.5	13.4	22.2	1.9	2.1
ReMEmbR	Llama3.1-8B	7 ¹	-	21.16	-	27.2	-	19.4	-	4.1
ReMEmbR	GPT-5.2	51 ¹	-	26.56	-	31.1	-	32.3	-	2.8
GenS	Qwen-2.5-VL-7B	8	16.6	22.3	22.6	25.5	13.6	28.1	2.9	2.8
ViaRL	Qwen-2.5-VL-7B	8	14.9	21.4	20.8	28.0	12.3	30.0	1.7	1.2
FocusGraph (ours)	Qwen-2.5-VL-7B	8	<u>15.5</u>	27.5	20.7	34.5	14.2	28.3	1.8	3.1

Table 2: Performance comparison across frame sampling methods and LLM settings (HourVideo).

Frame Selection Method	QA LLM	Frame Number	Overall						
			Navigation	Perception	Visual Reasoning	Summarization	Summarization	Summarization	Summarization
Uniform Sampling	Qwen-2.5-VL-7B	8	29.86	10.0	33.7	27.9	37.8		
Uniform Sampling	Qwen-2.5-VL-7B	16	31.22	15.0	36.8	27.5	43.9		
MaxInfo	Qwen-2.5-VL-7B	16	29.61	17.5	33.9	26.6	40.2		
ReMEmbR	Llama3.1-8B	8 ¹	24.28	17.5	24.54	27.47	0.0		
GenS	Qwen-2.5-VL-7B	8	32.9	27.5	34.5	31.8	37.8		
ViaRL	Qwen-2.5-VL-7B	8	32.23	17.5	33.4	31.0	43.9		
FocusGraph-s (ours)	Qwen-2.5-VL-7B	8	32.3 ± 0.1	24.2 ± 1.0	31.1 ± 0.5	32.1 ± 0.3	43.1 ± 1.0		
FocusGraph-m (ours)	Qwen-2.5-VL-7B	8	33.4 ± 0.5	21.7 ± 3.0	32.6 ± 0.6	33.6 ± 0.6	44.3 ± 1.4		

ViaRL [43] are LLM-based methods that reason over a sequence of uniformly sampled, low-resolution video frames, relying on raw visual appearance to guide temporal understanding. ReMEmbR [1] is an LLM-based retrieval-augmented generation (RAG) approach that employs an agent to iteratively retrieve and reason over visual evidence from memory. In contrast, MaxInfo [20] is a training-free baseline that selects frames by maximizing information content without reasoning. Finally, Uniform sampling serves as a standard key-frame sampling baseline, selecting frames at fixed temporal intervals without adaptivity.

Training details. We perform full supervised fine-tuning (SFT) of the Scene-Caption LLM selector on the GenS-Video-150K dataset [47] and an additional dataset containing 170K captions derived from our clip annotations on the same video subset as in GenS-Video-150K. We use AdamW with separate learning rates for the LLM backbone (1e-5) and adapters (1e-4) with a cosine annealing schedule. The LLM backbone is Qwen2.5-3B-Instruct [36]. Training is performed for one epoch using mixed-precision bfloat16 with an accumulated batch size of 128. Training is carried out on 4 NVIDIA A100 GPUs for 6 hours.

4.1 Results

Comparison with the state-of-the-art methods. Tab. 1 compares the performance of different frame selection (sampling) methods combined with various QA LLMs on the Finding Dory benchmark, reporting relaxed accuracy across different sets of tasks. Uniform sampling shows highly variable results depending on

¹ For ReMEmbR, frame number is the average number of documents retrieved from the database per query.

Table 3: Comparison of methods by token usage and inference time on HourVideo.

Method	Number of beams	Tokens per frame	Inference time, s
ReMEmbR	-	-	80
GenS	1	16	103
ViaRL	1	16	<u>2.6</u>
Scene-Caption LLM Selector-s (ours)	1	<1	0.6
Scene-Caption LLM Selector-m (ours)	5	<1	2.8
MaxInfo	-	-	0.038
PSFR (ours)	-	-	0.021

Table 4: Ablation study with explicit component inclusion.

Adapter type	Time range	PSFR	All	Single-Goal	Single-Goal	Multi-Goal
			Tasks	Spatial Tasks	Temporal Tasks	Tasks
GAT	×	×	13.9	19.3	11.3	1.7
MLP	×	×	13.9	19.1	11.9	1.4
MLP	×	✓	<u>15.4</u>	21.0	<u>12.9</u>	2.1
MLP	✓	✓	15.5	<u>20.7</u>	14.2	<u>2.0</u>

the LLM and number of frames, ranging from very low performance with Qwen-2.5-VL-7B at 8 frames to strong results with the proprietary models, especially when using 96 frames. Baseline methods such as MaxInfo, ReMEmbR, GenS, and ViaRL generally improve over low-frame uniform sampling. The proposed FocusGraph framework, using Qwen-2.5-VL-7B with 8 frames, outperforms ViaRL and achieves results close to GenS, while demonstrating significantly faster inference (see Tab. 3).

A visual comparison of the frames sampled by ViaRL, GenS and FocusGraph is provided in Fig. 3. The sampled sets vary significantly in their alignment with the ground truth. While ViaRL fails to sample any correct frames, GenS captures one, and FocusGraph successfully selects three frames that are present in the ground truth answer. When using Qwen-2.5-VL-7B for further frame selection, both GenS and FocusGraph identify a single correct frame.

We further compare FocusGraph with different frame sampling methods Tab. 2 on the HourVideo benchmark across multiple task categories. Uniform sampling with Qwen-2.5-VL-7B shows improved overall performance when increasing the number of frames from 8 to 16, particularly benefiting navigation and summarization. Among learned methods, GenS with only 8 frames achieves the highest overall scores. MaxInfo with 16 frames performs comparably to uniform sampling but does not surpass it overall, while FocusGraph (ours) demonstrates balanced performance across tasks with competitive performance with overall score close to GenS and outperforms ViaRL.

We compare our method with baseline methods in terms of token usage per frame and inference time in seconds (see Tab. 3). We separately measure the performance of the two components of our method: the Scene-Caption LLM Selector and the training-free PSFR, which runs on a CPU. Measurements for methods running on a GPU were conducted on an Nvidia RTX 4090. For the Scene-Caption LLM Selector, we report performance including the time required for a single question. ReMEmbR is an agent-based method and takes 80 s for inference, while GenS and ViaRL use 16 tokens per frame, with inference times of 103 s and 2.6 s, respectively. The proposed Scene-Caption LLM Selector significantly reduces token usage to less than 1 token per frame and achieves a much

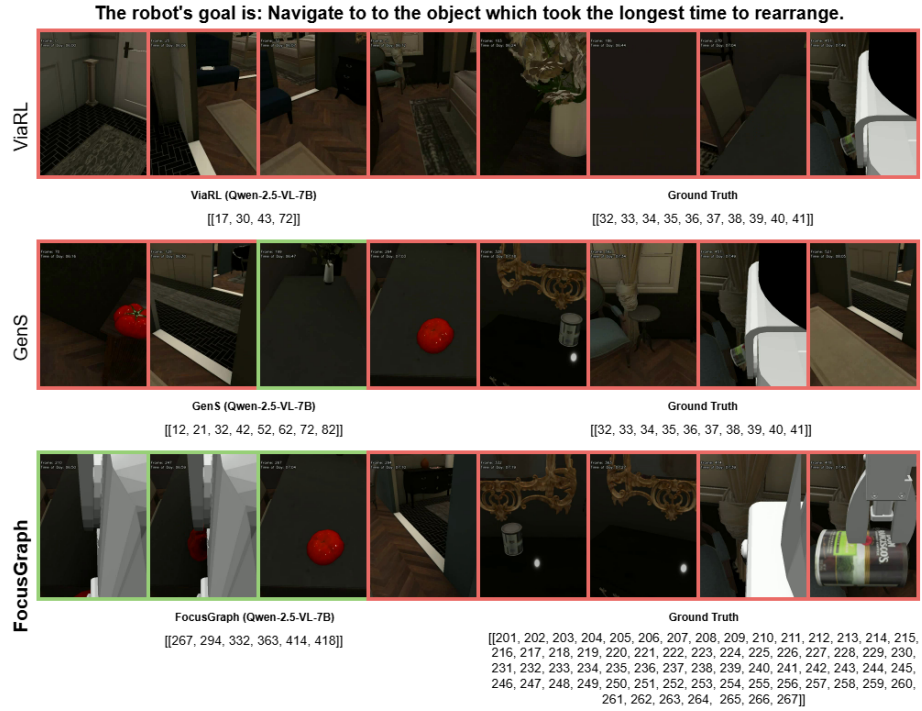


Fig. 3: Comparison of frame sampling methods (Finding Dory: episode 2, task 49). Green-bordered frames are present in the ground truth; red-bordered frames are not.

faster inference time of 0.6 s. When measuring the performance of MaxInfo and our PSFR, we measure the time required to process a single frame, as both methods select key frames independently of the question. PSFR, however, runs nearly twice as fast as MaxInfo, using only the CPU.

4.2 Ablation studies

To evaluate the contribution of each component in our model, we conduct a series of ablation studies.

Ablation study on FocusGraph component inclusion. Tab. 4 presents an ablation study analyzing the impact of adapter type, temporal range modeling, and PSFR on task performance. Without PSFR, both GAT and MLP adapters achieve similar results. Enabling PSFR consistently improves performance, increasing overall scores to 15.4. Incorporating both PSFR and time-range modeling yields the best overall performance, with notable gains on temporal tasks. Overall, PSFR contributes the largest improvement, while time-range modeling further enhances temporal task performance.

Ablation on frame selection: PSFR selector objectives. We evaluate the query-agnostic keyframe selector, limited to at most $K=16$ frames per

Table 5: Ablation of program-evolved keyframe selectors under a fixed budget of $K=16$ frames. FD denotes full-video FindingDory oracle evaluation. GenS denotes GenS-Videos-150K evaluation, where w-Inter is the weighted-intersection metric used by the GenS protocol. $F_{\sqrt{2}}$ is F_{β} with $\beta = \sqrt{2}$. Time reports CPU-only selector execution time per video as mean \pm std over 100 FindingDory validation videos.

Method	FD			GenS		Time (s)
	Inter	Incl	$F_{\sqrt{2}}$	w-Inter	Incl	$\mu \pm \sigma$
Uniform	0.111	0.715	0.0136	0.470	0.890	–
Evolved on Intersection (FindingDory)	0.212	0.645	0.0289	0.449	0.803	1.371 ± 0.965
Evolved on Inclusion (FindingDory) (PSFR)	0.1678	0.866	0.0217	0.489	0.884	0.065 ± 0.025
Evolved on $F_{\sqrt{2}}$ (FindingDory)	0.181	0.834	0.0250	0.426	0.770	0.038 ± 0.023
Evolved on Weighted Intersection (GenS)	0.100	0.516	0.0110	0.521	0.858	0.013 ± 0.005

clip, independently from downstream MLLM reasoning using an oracle protocol based on frame-level annotations (see Tab. 5). For each QA instance, the selector outputs a subset of frames, and performance is measured against all valid ground-truth evidence sets. We report three complementary scores. Intersection (Inter) is precision-oriented and penalizes over-selection with worst-case aggregation across valid ground-truth sets. Inclusion (Incl) measures whether at least one supporting frame is retrieved for each valid grounding and reflects evidence coverage. $F_{\sqrt{2}}$ is an F_{β} score with $\beta = \sqrt{2}$ that emphasizes coverage while still discouraging redundant selection. We compute these metrics on full FindingDory videos (FD). On GenS-Videos-150K (GenS), we report the protocol weighted intersection (w-Inter) alongside inclusion. We also report CPU-only selector runtime as mean \pm std execution time per video over 100 FindingDory validation videos.

Optimizing directly for intersection yields the strongest precision on FindingDory, achieving the best FD Inter (0.212) and the highest FD $F_{\sqrt{2}}$ (0.0289), but it substantially reduces coverage compared to the inclusion-optimized variant (FD Incl 0.645 vs 0.866). In contrast, the inclusion-optimized selector, which we use as PSFR, achieves the strongest evidence coverage on FindingDory (FD Incl 0.866) while retaining competitive precision (FD Inter 0.1678), making it a more reliable choice when retrieving at least one annotated evidence frame per acceptable grounding is the priority. Optimizing $F_{\sqrt{2}}$ produces a balanced selector that improves over the uniform baseline on FD $F_{\sqrt{2}}$ (0.0250 vs 0.0136) while maintaining strong inclusion (0.834). A selector evolved on GenS generalizes best to GenS, reaching the top w-Inter (0.521) with high Incl (0.858), but it aligns poorly with FindingDory evidence (FD Inter 0.100, Incl 0.516). Runtime differs markedly across objectives: the intersection-optimized program is the slowest (1.371 ± 0.965 s), while PSFR remains lightweight (0.065 ± 0.025 s) and the GenS-evolved program is the fastest among non-trivial selectors (0.013 ± 0.005 s). Overall, the evolved objective controls the precision–coverage trade-off under a fixed frame budget, while CPU overhead remains small relative to MLLM inference.

5 Conclusion

In conclusion, we have presented FocusGraph, a novel framework that addresses the challenges of long-video question answering in embodied environments. By combining query-conditioned frame selection with a hierarchical graph-based scene representation, our approach efficiently captures object interactions and temporal dependencies over extended horizons. This allows for accurate reasoning without the computational burden of processing every frame. Extensive evaluations on egocentric LVQA benchmarks demonstrate that FocusGraph achieves state-of-the-art accuracy while significantly improving inference efficiency. Our work underscores the value of structured, selective temporal abstraction in embodied video understanding and opens new avenues for scalable, intelligent agents capable of reasoning over complex, long-horizon visual experiences. Additionally, we demonstrate that the selection of semantically relevant video episodes can be effectively decoupled from keyframe extraction, which is driven by low-level visual properties, enabling a principled separation between semantic reasoning and visual redundancy reduction.

References

1. Anwar, A., Welsh, J., Biswas, J., Pouya, S., Chang, Y.: Remembr: Building and reasoning over long-horizon spatio-temporal memory for robot navigation. In: 2025 IEEE International Conference on Robotics and Automation (ICRA). pp. 2838–2845. IEEE (2025)
2. Bai, S., Chen, K., Liu, X., Wang, J., Ge, W., Song, S., Dang, K., Wang, P., Wang, S., Tang, J., et al.: Qwen2. 5-vl technical report. arXiv preprint arXiv:2502.13923 (2025)
3. Canny, J.: A computational approach to edge detection. *IEEE Transactions on pattern analysis and machine intelligence* (6), 679–698 (2009)
4. Chandrasegaran, K., Gupta, A., Hadzic, L.M., Kota, T., He, J., Eyzaguirre, C., Durante, Z., Li, M., Wu, J., Fei-Fei, L.: Hourvideo: 1-hour video-language understanding. *Advances in Neural Information Processing Systems* **37**, 53168–53197 (2024)
5. Cheng, Z., Tu, Y., Li, R., Dai, S., Hu, J., Hu, S., Li, J., Shi, Y., Yu, T., Chen, W., et al.: Embodiedeval: Evaluate multimodal llms as embodied agents. arXiv preprint arXiv:2501.11858 (2025)
6. Damen, D., Doughty, H., Farinella, G.M., Fidler, S., Furnari, A., Kazakos, E., Moltisanti, D., Munro, J., Perrett, T., Price, W., et al.: Scaling egocentric vision: The epic-kitchens dataset. In: *Proceedings of the European conference on computer vision (ECCV)*. pp. 720–736 (2018)
7. Fan, S., Guo, M.H., Yang, S.: Agentic keyframe search for video question answering. arXiv preprint arXiv:2503.16032 (2025)
8. Fan, Y., Ma, X., Su, R., Guo, J., Wu, R., Chen, X., Li, Q.: Embodied videoagent: Persistent memory from egocentric videos and embodied sensors enables dynamic scene understanding. In: *Proceedings of the IEEE/CVF International Conference on Computer Vision*. pp. 6342–6352 (2025)

9. Gothe, S.V., Agarwal, V., Ghosh, S., Vachhani, J.R., Kashyap, P., Raja, B.R.K.: What's in the flow? exploiting temporal motion cues for unsupervised generic event boundary detection. In: Proceedings of the IEEE/CVF Winter Conference on Applications of Computer Vision. pp. 6941–6950 (2024)
10. Grauman, K., Westbury, A., Byrne, E., Chavis, Z., Furnari, A., Girdhar, R., Hamburger, J., Jiang, H., Liu, M., Liu, X., et al.: Ego4d: Around the world in 3,000 hours of egocentric video. In: Proceedings of the IEEE/CVF conference on computer vision and pattern recognition. pp. 18995–19012 (2022)
11. Guo, W., Chen, Z., Wang, S., He, J., Xu, Y., Ye, J., Sun, Y., Xiong, H.: Logic-in-frames: Dynamic keyframe search via visual semantic-logical verification for long video understanding. arXiv preprint arXiv:2503.13139 (2025)
12. Guo, Y., Siddiqui, F., Zhao, Y., Chellappa, R., Lo, S.Y.: Stimuvar: Spatiotemporal stimuli-aware video affective reasoning with multimodal large language models. *International Journal of Computer Vision* **133**(9), 6456–6472 (2025). <https://doi.org/10.1007/s11263-025-02495-3>
13. He, B., Li, H., Jang, Y.K., Jia, M., Cao, X., Shah, A., Shrivastava, A., Lim, S.N.: Ma-lmm: Memory-augmented large multimodal model for long-term video understanding. In: Proceedings of the IEEE/CVF Conference on Computer Vision and Pattern Recognition. pp. 13504–13514 (2024)
14. Huimin Zeng, Jiacheng Li, Z.X.: Plug-and-play versatile compressed video enhancement. arXiv preprint arXiv:2504.15380v1 (2025), <https://arxiv.org/abs/2504.15380v1>
15. Khanna, M., Mao, Y., Jiang, H., Haresh, S., Shacklett, B., Batra, D., Clegg, A., Undersander, E., Chang, A.X., Savva, M.: Habitat synthetic scenes dataset (hssd-200): An analysis of 3d scene scale and realism tradeoffs for objectgoal navigation. In: Proceedings of the IEEE/CVF Conference on Computer Vision and Pattern Recognition. pp. 16384–16393 (2024)
16. Khanna, M., Ramrakhya, R., Chhablani, G., Yenamandra, S., Gervet, T., Chang, M., Kira, Z., Chaplot, D.S., Batra, D., Mottaghi, R.: Goat-bench: A benchmark for multi-modal lifelong navigation. In: Proceedings of the IEEE/CVF Conference on Computer Vision and Pattern Recognition. pp. 16373–16383 (2024)
17. Kou, L., Ni, F., HAO, J., Peilong, H., Liu, J., Cui, H., Liu, R., ZHENG, Y.: Roboannotatorx: A comprehensive and universal annotation framework for accurate understanding of long-horizon robot demonstration (2025), <https://iccv.thecvf.com/virtual/2025/poster/2215>
18. Lars Doorenbos, Federico Spurio, J.G.: Video panels for long video understanding. arXiv preprint arXiv:2509.23724v1 (2025), <https://arxiv.org/abs/2509.23724v1>
19. Li, P., Song, P., Li, W., Yao, H., Guo, W., Xu, Y., Liu, D., Xiong, H.: See&trek: Training-free spatial prompting for multimodal large language model. In: The Thirty-ninth Annual Conference on Neural Information Processing Systems
20. Li, P., Abdullaeva, I., Gambashidze, A., Kuznetsov, A., Oseledets, I.: Maxinfo: A training-free key-frame selection method using maximum volume for enhanced video understanding. arXiv preprint arXiv:2502.03183 (2025)
21. Li, X., Wang, Y., Yu, J., Zeng, X., Zhu, Y., Huang, H., Gao, J., Li, K., He, Y., Wang, C., et al.: Videochat-flash: Hierarchical compression for long-context video modeling. arXiv preprint arXiv:2501.00574 (2024)
22. Li, Y., Wang, C., Jia, J.: Llama-vid: An image is worth 2 tokens in large language models. In: European Conference on Computer Vision. pp. 323–340. Springer (2024)

23. Ling, T., Shi, S., Wang, D.: Accelerating long video understanding via compressed scene graph-enabled chain-of-thought. In: Proceedings of the 33rd ACM International Conference on Multimedia. pp. 965–974 (2025)
24. Linok, S., Semenov, V., Trunova, A., Bulichev, O., Yudin, D.: Dygenc: Encoding a sequence of textual scene graphs to reason and answer questions in dynamic scenes. arXiv preprint arXiv:2505.03581 (2025)
25. Long, L., He, Y., Ye, W., Pan, Y., Lin, Y., Li, H., Zhao, J., Li, W.: Seeing, listening, remembering, and reasoning: A multimodal agent with long-term memory. arXiv preprint arXiv:2508.09736 (2025)
26. Lucas, B.D., Kanade, T.: An iterative image registration technique with an application to stereo vision. In: IJCAI’81: 7th international joint conference on Artificial intelligence. vol. 2, pp. 674–679 (1981)
27. Mao, J., Jiang, W., Wang, X., Feng, Z., Lyu, Y., Liu, H., Zhu, Y.: Dynamic multistep reasoning based on video scene graph for video question answering. In: Proceedings of the 2022 Conference of the North American Chapter of the Association for Computational Linguistics: Human Language Technologies. pp. 3894–3904 (2022)
28. Nguyen, T.T., Nguyen, P., Cothren, J., Yilmaz, A., Luu, K.: Hyperglm: Hypergraph for video scene graph generation and anticipation. In: Proceedings of the Computer Vision and Pattern Recognition Conference. pp. 29150–29160 (2025)
29. Qiu, H., Gao, M., Qian, L., Pan, K., Yu, Q., Li, J., Wang, W., Tang, S., Zhuang, Y., Chua, T.S.: Step: Enhancing video-llms’ compositional reasoning by spatio-temporal graph-guided self-training. In: Proceedings of the Computer Vision and Pattern Recognition Conference. pp. 3284–3294 (2025)
30. Rodin, I., Furnari, A., Min, K., Tripathi, S., Farinella, G.M.: Action scene graphs for long-form understanding of egocentric videos. In: Proceedings of the IEEE/CVF Conference on Computer Vision and Pattern Recognition. pp. 18622–18632 (2024)
31. Sharma, A.: Openevolve: an open-source evolutionary coding agent (2025), <https://github.com/algorithmicsuperintelligence/openevolve>
32. Shen, X., Xiong, Y., Zhao, C., Wu, L., Chen, J., Zhu, C., Liu, Z., Xiao, F., Varadarajan, B., Bordes, F., et al.: Longvu: Spatiotemporal adaptive compression for long video-language understanding. In: Forty-second International Conference on Machine Learning
33. Shi, J., et al.: Good features to track. In: 1994 Proceedings of IEEE conference on computer vision and pattern recognition. pp. 593–600. IEEE (1994)
34. Tang, C., Han, Z., Sun, H., Zhou, S., Zhang, X., Wei, X., Yuan, Y., Zhang, H., Xu, J., Sun, H.: Tspo: Temporal sampling policy optimization for long-form video language understanding. arXiv preprint arXiv:2508.04369 (2025)
35. Tang, X., Qiu, J., Xie, L., Tian, Y., Jiao, J., Ye, Q.: Adaptive keyframe sampling for long video understanding. In: Proceedings of the Computer Vision and Pattern Recognition Conference. pp. 29118–29128 (2025)
36. Team, Q.: Qwen2.5-vl (January 2025), <https://qwenlm.github.io/blog/qwen2.5-vl/>
37. Wang, K., Lin, M.: Test-time temporal sampling for efficient mllm video understanding. arXiv preprint arXiv:2511.17945 (2025)
38. Wang, S., Chen, G., Huang, D.a., Li, Z., Li, M., Li, G., Alvarez, J.M., Zhang, L., Yu, Z.: Videoitg: Multimodal video understanding with instructed temporal grounding. arXiv preprint arXiv:2507.13353 (2025)
39. Wang, Y., Li, K., Li, X., Yu, J., He, Y., Chen, G., Pei, B., Zheng, R., Wang, Z., Shi, Y., et al.: Internvideo2: Scaling foundation models for multimodal video un-

- derstanding. In: European Conference on Computer Vision. pp. 396–416. Springer (2024)
40. Wu, H., Li, D., Chen, B., Li, J.: Longvideobench: A benchmark for long-context interleaved video-language understanding. *Advances in Neural Information Processing Systems* **37**, 28828–28857 (2024)
 41. Wu, R., Ma, X., Ci, H., Fan, Y., Wang, Y., Zhao, H., Li, Q., Wang, Y.: Longvitu: Instruction tuning for long-form video understanding. *arXiv preprint arXiv:2501.05037* (2025)
 42. Xie, Q., Min, S.Y., Ji, P., Yang, Y., Zhang, T., Xu, K., Bajaj, A., Salakhutdinov, R., Johnson-Roberson, M., Bisk, Y.: Embodied-rag: General non-parametric embodied memory for retrieval and generation. *arXiv preprint arXiv:2409.18313* (2024)
 43. Xu, Z., Dai, Q., Xie, T., Yang, Y., Qiu, K., Chen, D., Wu, Z., Luo, C.: Viarl: Adaptive temporal grounding via visual iterated amplification reinforcement learning. *arXiv preprint arXiv:2505.15447* (2025)
 44. Yadav, K., Ali, Y., Gupta, G., Gal, Y., Kira, Z.: Findingdory: A benchmark to evaluate memory in embodied agents. *arXiv preprint arXiv:2506.15635* (2025)
 45. Yang, Y., Zhao, Z., Shukla, S.N., Singh, A., Mishra, S.K., Zhang, L., Ren, M.: Streammem: Query-agnostic kv cache memory for streaming video understanding. *arXiv preprint arXiv:2508.15717* (2025)
 46. Yang, Y., Yang, H., Zhou, J., Chen, P., Zhang, H., Du, Y., Gan, C.: 3d-mem: 3d scene memory for embodied exploration and reasoning. In: *Proceedings of the Computer Vision and Pattern Recognition Conference*. pp. 17294–17303 (2025)
 47. Yao, L., Wu, H., Ouyang, K., Zhang, Y., Xiong, C., Chen, B., Sun, X., Li, J.: Generative frame sampler for long video understanding. *arXiv preprint arXiv:2503.09146* (2025)
 48. Ye, H., Zhang, H., Daxberger, E., Chen, L., Lin, Z., Li, Y., Zhang, B., You, H., Xu, D., Gan, Z., et al.: Mm-ego: Towards building egocentric multimodal llms for video qa. *arXiv preprint arXiv:2410.07177* (2024)
 49. Yuan, C., Yang, Y., Yang, Y., Cheng, Z.: Date: Dynamic absolute time enhancement for long video understanding. *arXiv preprint arXiv:2509.09263v1* (2025), <https://arxiv.org/abs/2509.09263v1>
 50. Zellers, R., Lu, J., Lu, X., Yu, Y., Zhao, Y., Salehi, M., Kusupati, A., Hessel, J., Farhadi, A., Choi, Y.: Merlot reserve: Neural script knowledge through vision and language and sound. In: *Proceedings of the IEEE/CVF conference on computer vision and pattern recognition*. pp. 16375–16387 (2022)
 51. Zhang, H., Li, X., Bing, L.: Video-llama: An instruction-tuned audio-visual language model for video understanding. *arXiv preprint arXiv:2306.02858* (2023)
 52. Zhang, P., Zhang, K., Li, B., Zeng, G., Yang, J., Zhang, Y., Wang, Z., Tan, H., Li, C., Liu, Z.: Long context transfer from language to vision. *arXiv preprint arXiv:2406.16852* (2024)
 53. Zhang, S., Yang, J., Yin, J., Luo, Z., Luan, J.: Q-frame: Query-aware frame selection and multi-resolution adaptation for video-llms. *arXiv preprint arXiv:2506.22139* (2025)
 54. Zhong, Y., Liu, Z., Li, Y., Wang, L.: Aim: Adaptive inference of multi-modal llms via token merging and pruning. *arXiv preprint arXiv:2412.03248* (2025), <https://arxiv.org/abs/2412.03248>
 55. Zhu, Z., Xu, H., Luo, Y., Liu, Y., Sarkar, K., Yang, Z., You, Y.: Focus: Efficient keyframe selection for long video understanding. *arXiv preprint arXiv:2510.27280* (2025)

56. Zong, L., Zhai, X., Liu, X., Liang, W., Zhang, X., Xu, B.: Structuring video semantics with temporal triplets for zero-shot video question answering. In: Proceedings of the 34th ACM International Conference on Information and Knowledge Management. pp. 5545–5549 (2025)